Supplement of Biogeosciences, 21, 1549–1562, 2024
https://doi.org/10.5194/bg-21-1549-2024-supplement

Biogeosciences Open Access EGU

Supplement of

Thermal stratification and meromixis in four dilute temperate zone lakes

Elizabeth D. Swanner et al.

Correspondence to: Elizabeth D. Swanner (eswanner@iastate.edu)

Supplement for Thermal stratification and meromixis in four dilute temperate zone lakes

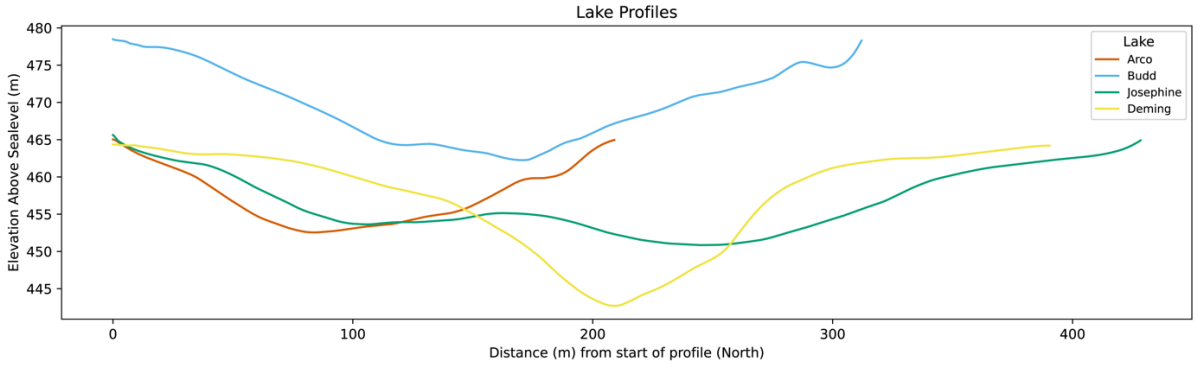

Fig. S1. Profiles of the lakes (in meters above mean sea level) along the fence diagrams in Fig. 1.

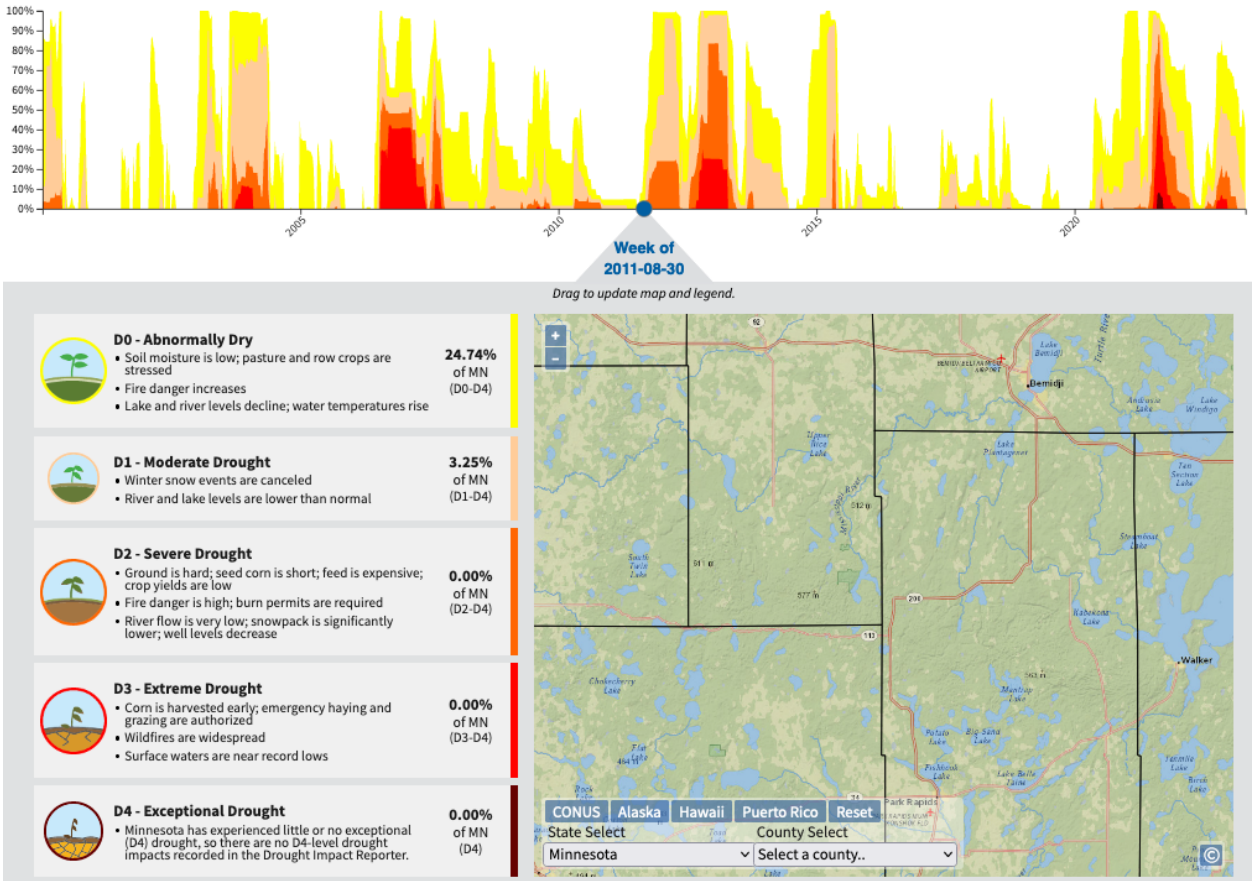

Fig. S2. Historical drought information for the counties encompassing Itasca State Park during the period of 2000-2023. Graphics were generated by the National Integrated Drought Information System.

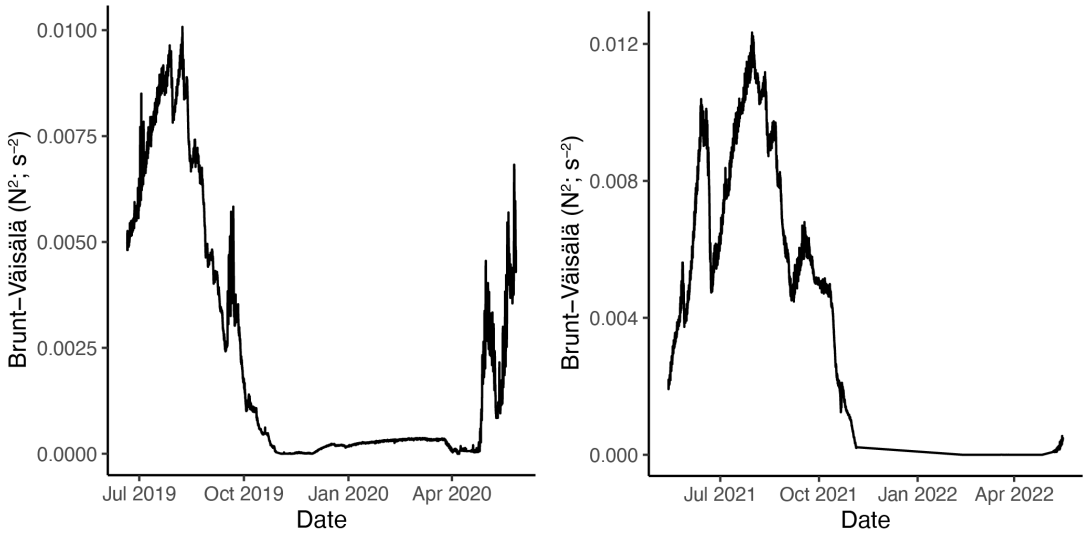

Fig. S3. The Brunt-Väisälä or buoyancy frequency (N^2, s^{-2}), calculated from the temperature time series for Deming Lake from June 2019 to May 2020 (left), and Arco Lake from May 2021 to May 2022 (right). Higher values indicate greater stability.

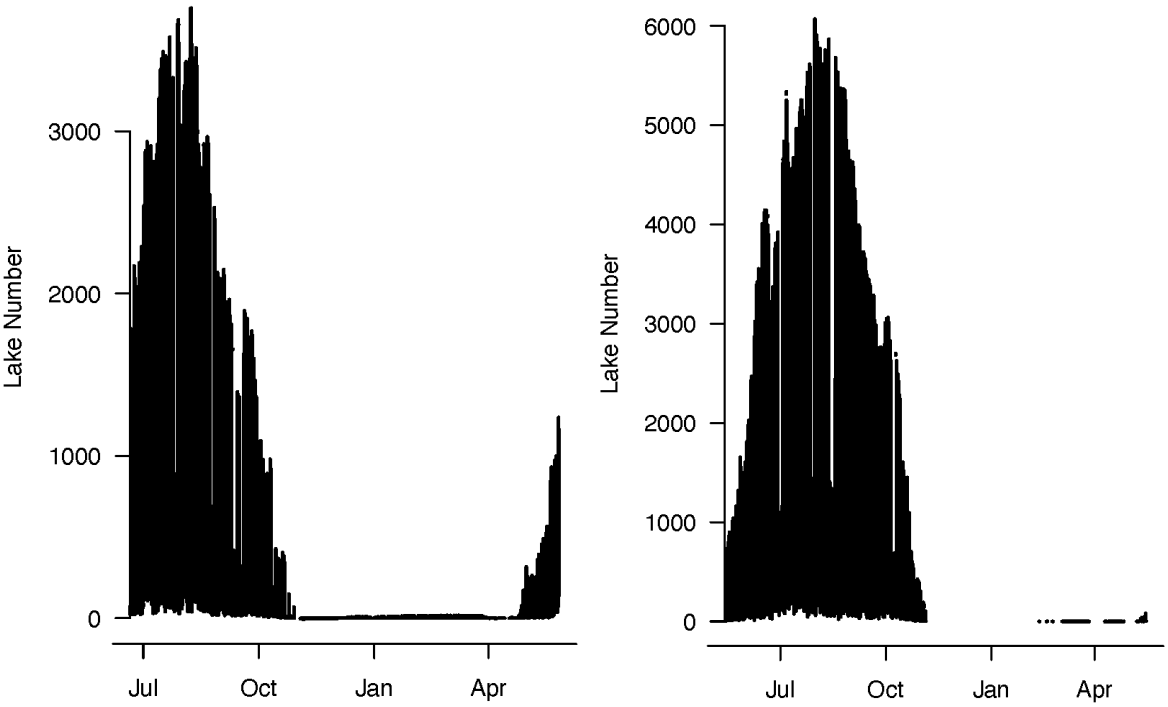

Fig. S4. The dimensionless lake number was calculated using wind speeds from the ITCM5 weather station and the temperature time series for Deming Lake from June 2019 to May 2020 (left), and Arco Lake from May 2021 to May 2022 (right). Higher values indicate greater stability.

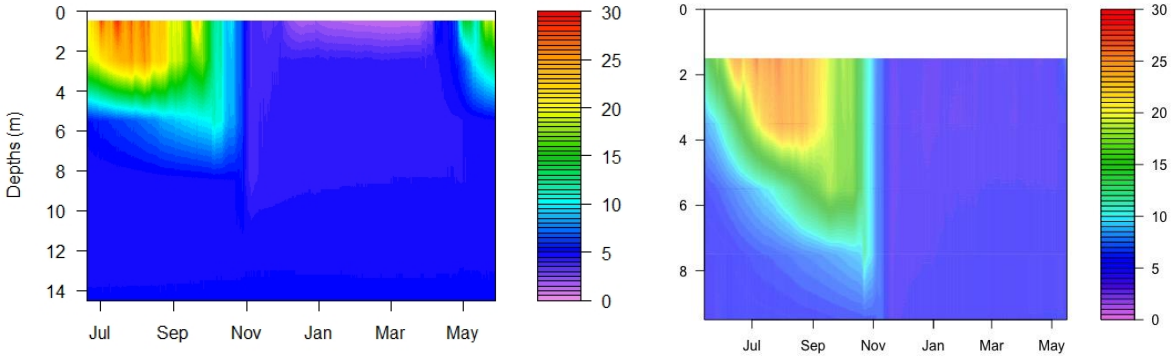

Fig. S5. Deming Lake temperatures (°C) from June 2019 to May 2020 (left). Arco Lake temperatures (°C) from May 2021 to May 2022 (right).

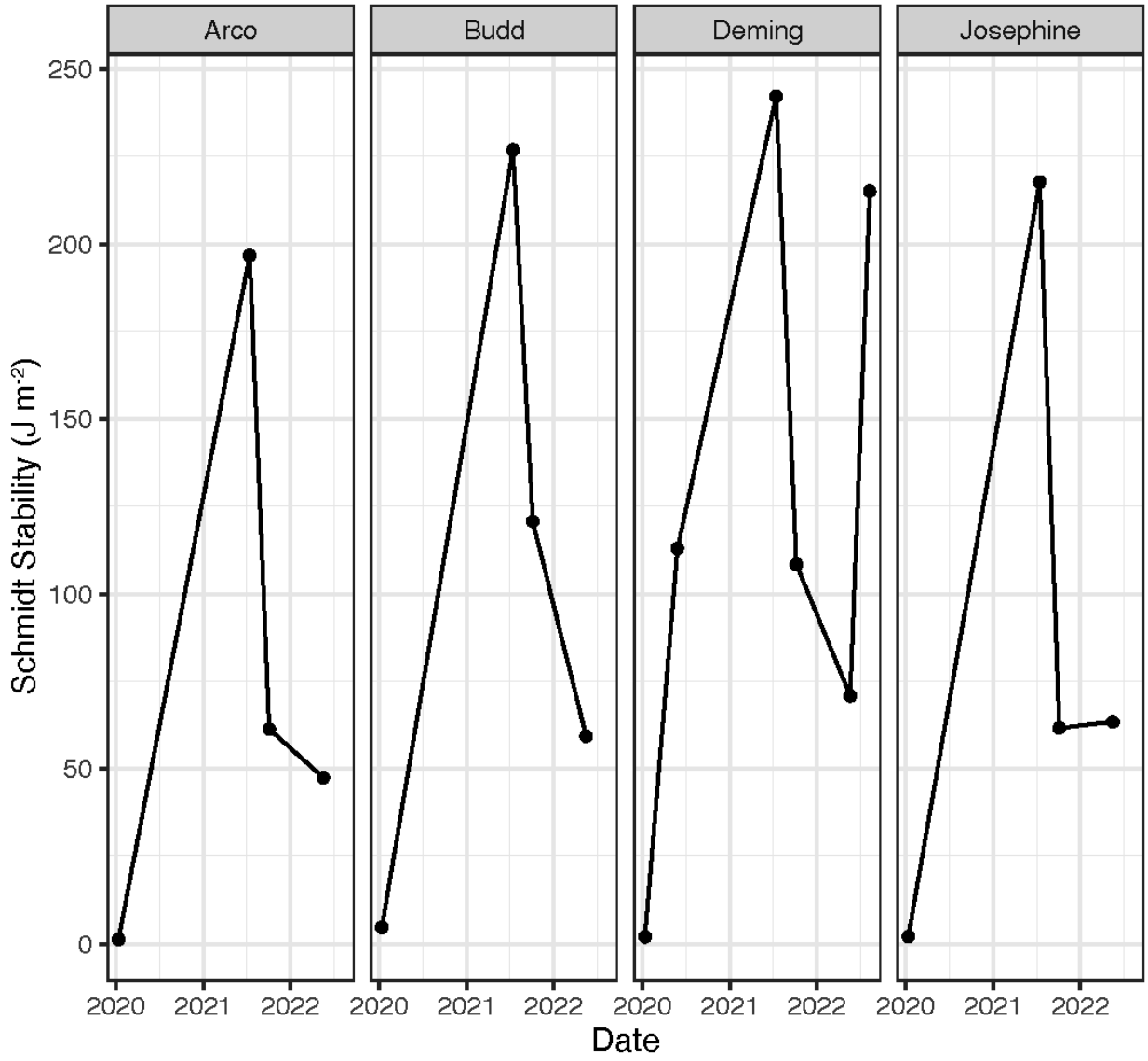

Fig S6. Plots of Schmidt Stability for each of the four study lakes from January 2021 to August 2022. Higher values indicate greater stability.

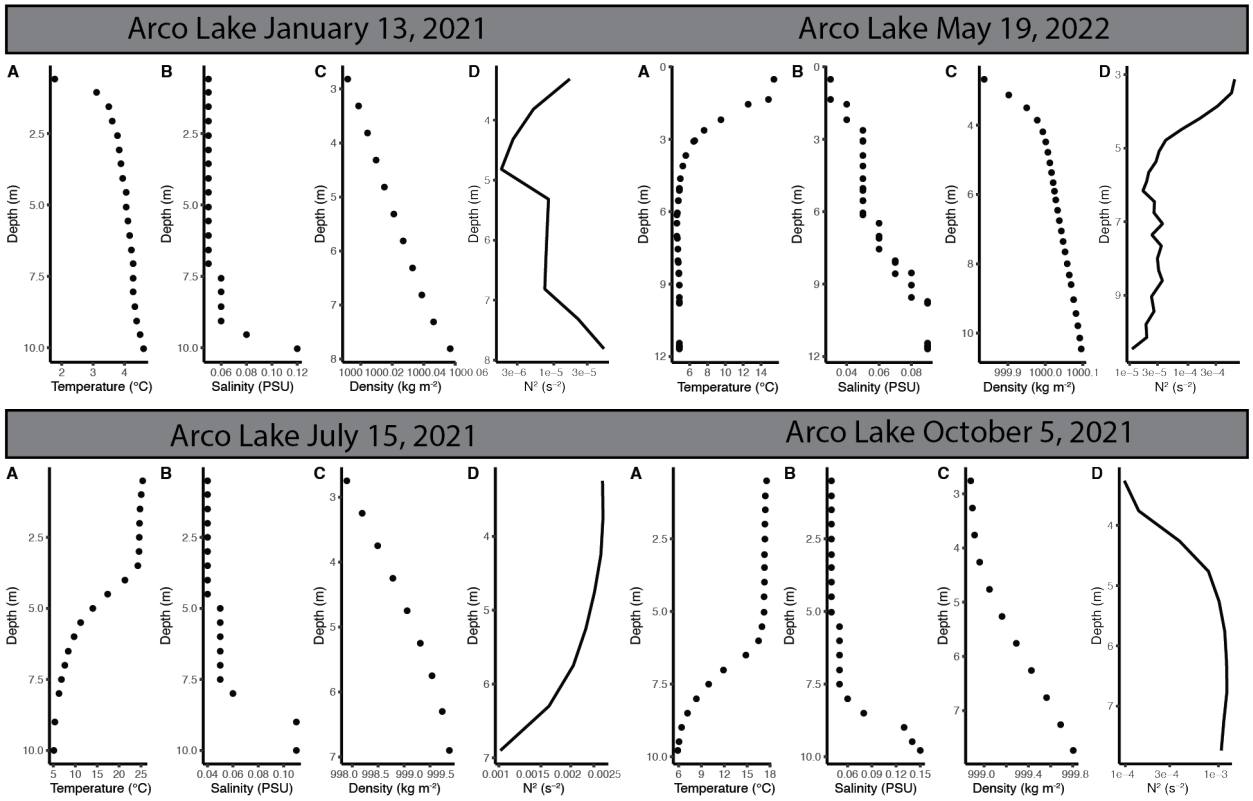

Fig. S7. The Brunt-Väisälä or buoyancy frequency (N^2, s^{-2}), calculated from the temperature and salinity profiles from Arco Lake from January 2021 to May 2022. Higher values indicate greater stability.

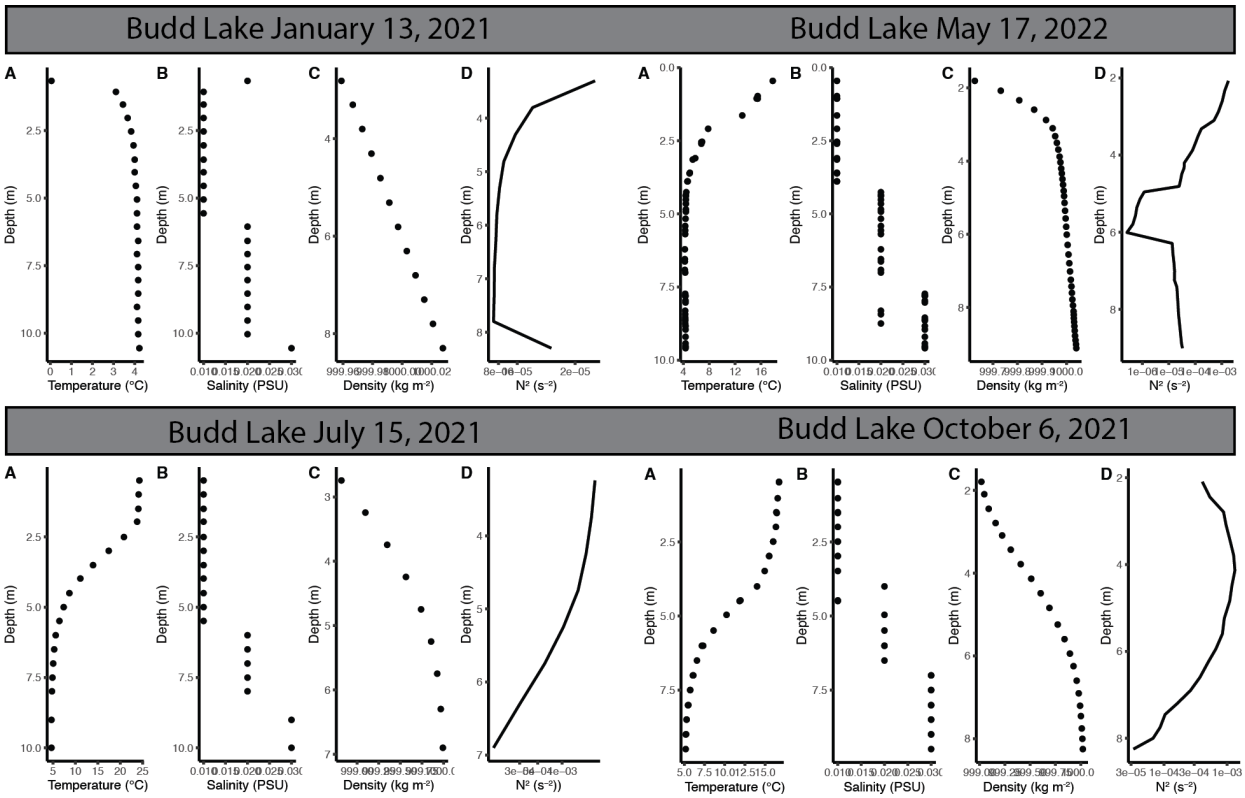

Fig. S8. The Brunt-Väisälä or buoyancy frequency (N^2, s^{-2}), calculated from the temperature and salinity profiles from Budd Lake from January 2021 to May 2022. Higher values indicate greater stability.

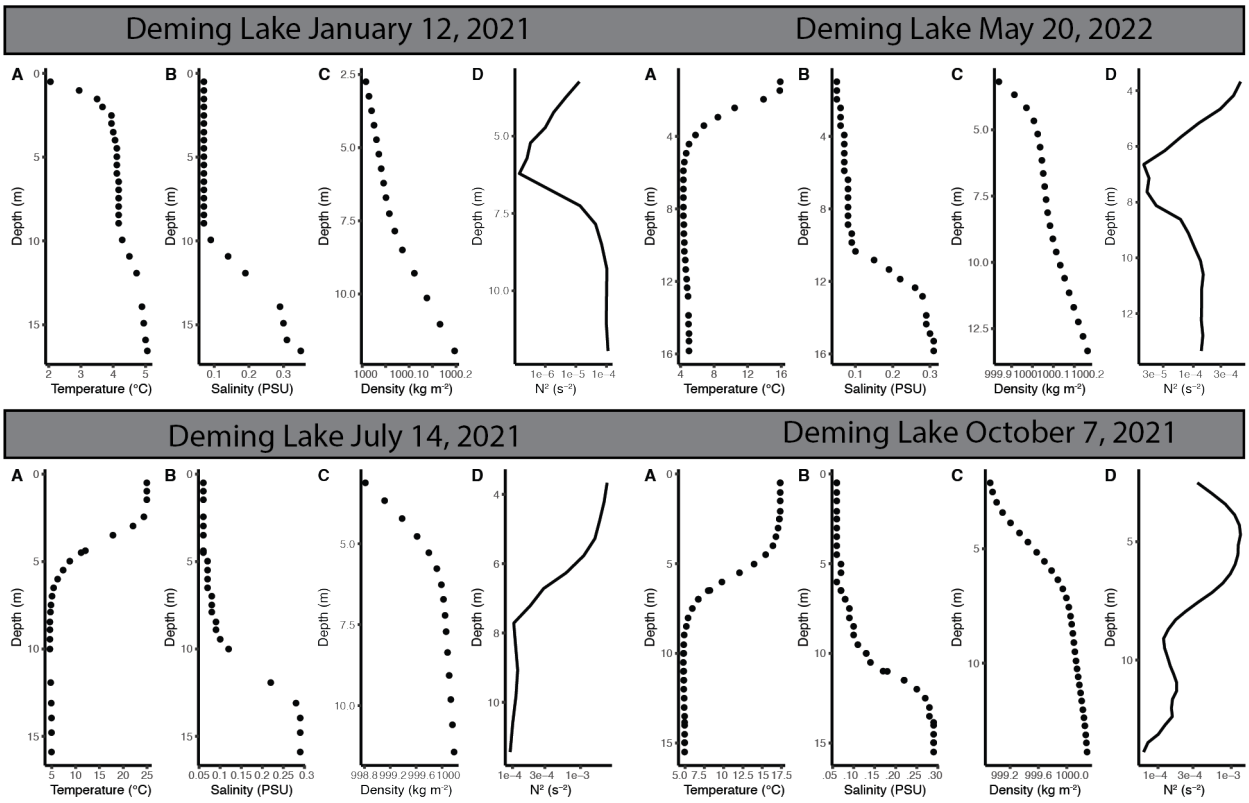

Fig. S9. The Brunt-Väisälä or buoyancy frequency (N^2, s^{-2}), calculated from the temperature and salinity profiles from Deming Lake from January 2021 to May 2022. Higher values indicate greater stability.

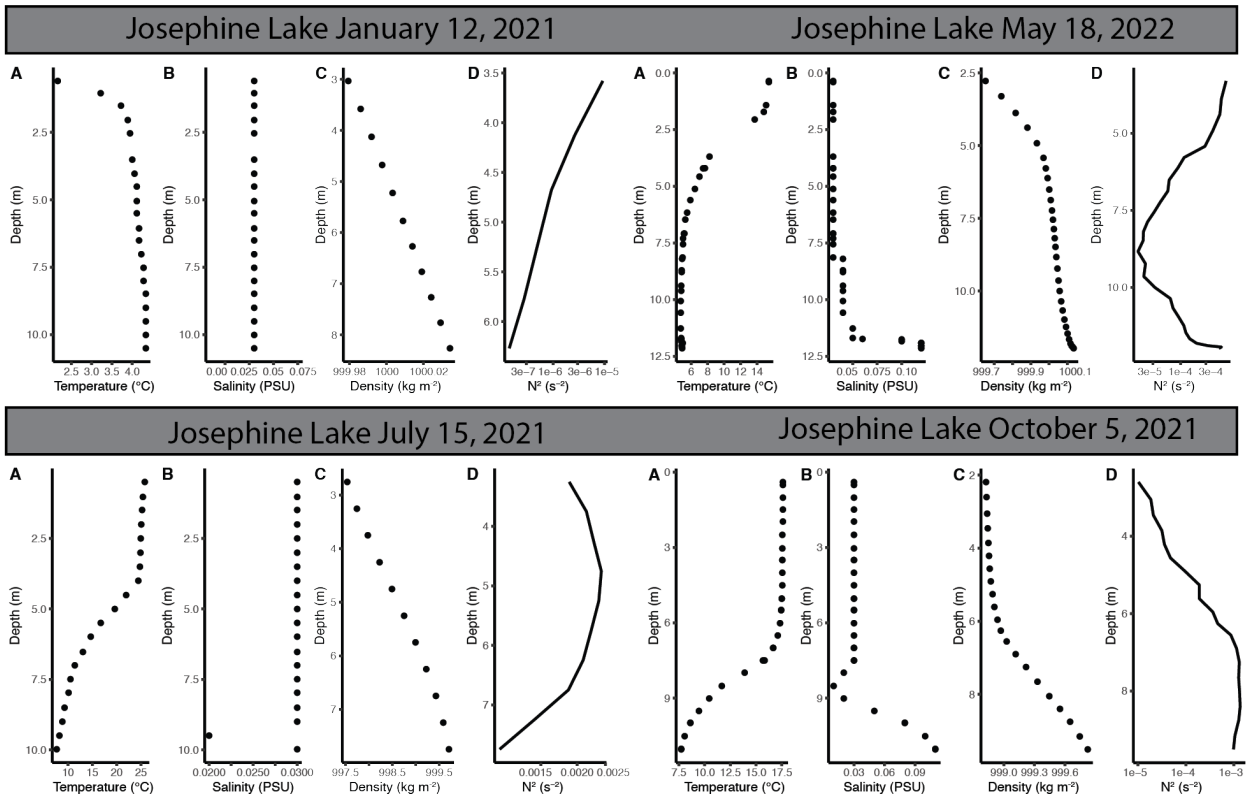

Fig. S10. The Brunt-Väisälä or buoyancy frequency (N^2, s^{-2}), calculated from the temperature and salinity profiles from Josephine Lake from January 2021 to May 2022. Higher values indicate greater stability.

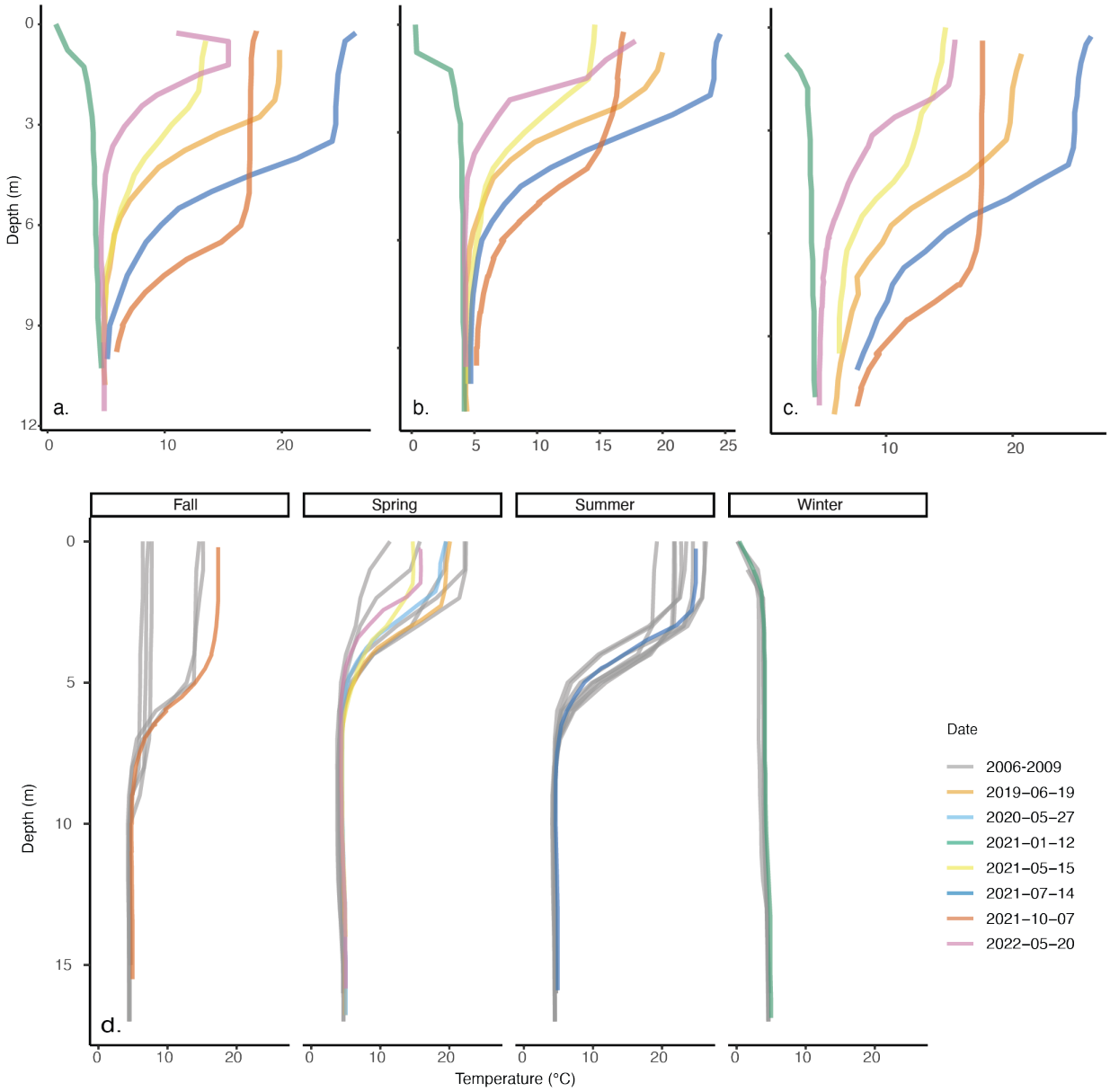

Fig. S11. Temperature profiles of a) Arco Lake, b) Budd Lake, c) Josephine Lake, and d) Deming Lake. For Deming Lake, seasons were classified according to solstice and equinox dates.

Table S1. Water color in mg Pt L-1. The depths of individual samples (in meters) are given in parentheses.

	Arco	Budd	Deming	Josephine
Depth 1	1.4 (4)	32.87 (2)	8.0 (3.5)	3.1 (2)
Depth 2	3.1 (5)	27.9 (4.5)	8.0 (4.5)	1.4 (4.5)
Depth 3	4.71 (5.5)	24.6 (9)	8.0 (5)	1.4 (9)

Average	3.1	28.4	8.0	2.0
Standard dev.	1.7	4.2	0	1.0

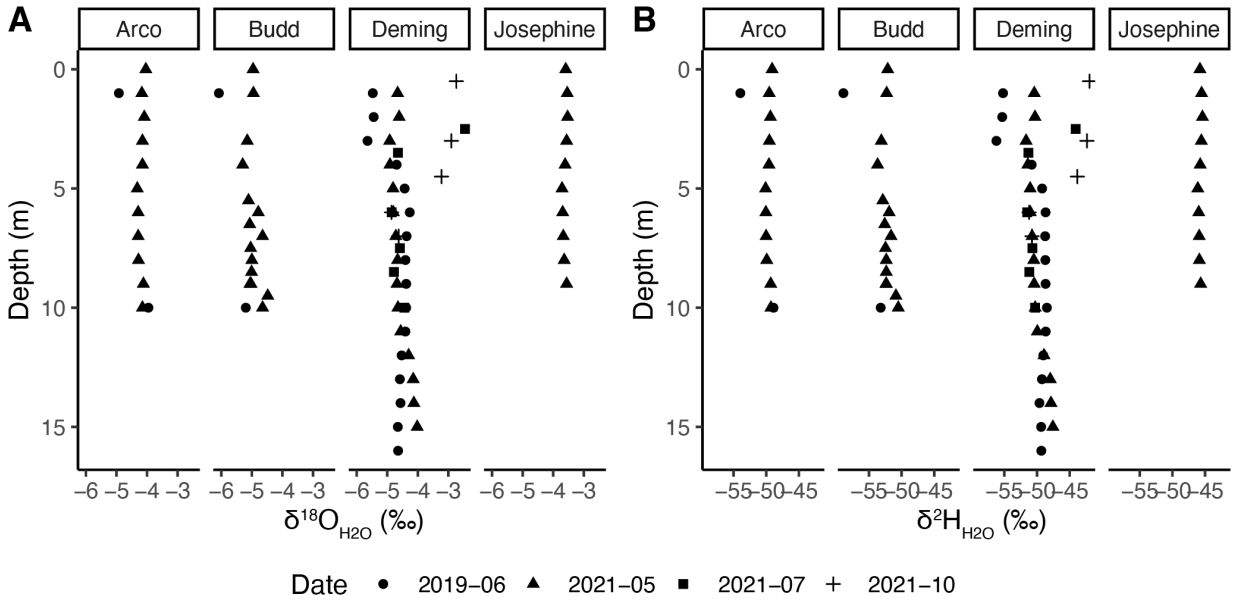

Fig. S12. Trends in $\delta^{18}O_{H2O}$ and $\delta^{2}H_{H2O}$ with depth in the four study lakes. Deming was the only lake sampled in all seasons. Analytical precision is within the symbol size.

Table S2. Stable isotopes of spring and bog water.

Site Name	Latitude	Longitude	$\delta^{18}O_{H2O}$ (‰)	$\delta^{2}H_{H2O}$ (‰)
Deming Bog	47.169440	-95.167162	-6.83	-10.90
Nicollet Creek	47.193874	-95.230539	-10.90	-81.36
Elk3	47.190478	-95.211350	-10.23	-77.36
Elk4	47.190478	-95.211350	-9.34	-73.92

The combined uncertainty (analytical uncertainty and average correction factor) for $\delta^{18}O$ is ± 0.04‰ VSMOW) and $\delta^{2}H$ is ± 0.25‰ (VSMOW), respectively.

Fig. S13. Left: marsh marigold in boggy areas around Deming Lake with 3x4 inch field notebook for scale. Right: iron mineralization at Elk springs.

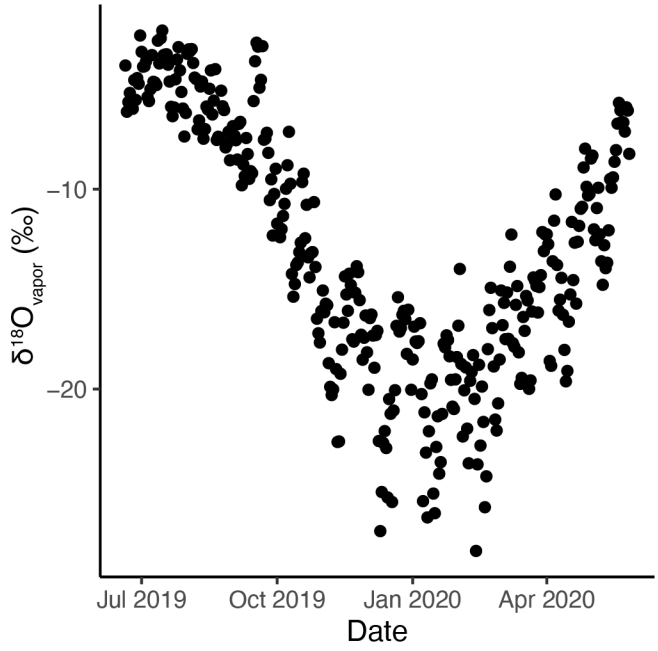

Fig. S14. The range of $\delta^{18}O_{H2O}$ calculated for water vapor based on temperature records from the ITCM5 station calculated according to Engel & Magner, 2019.

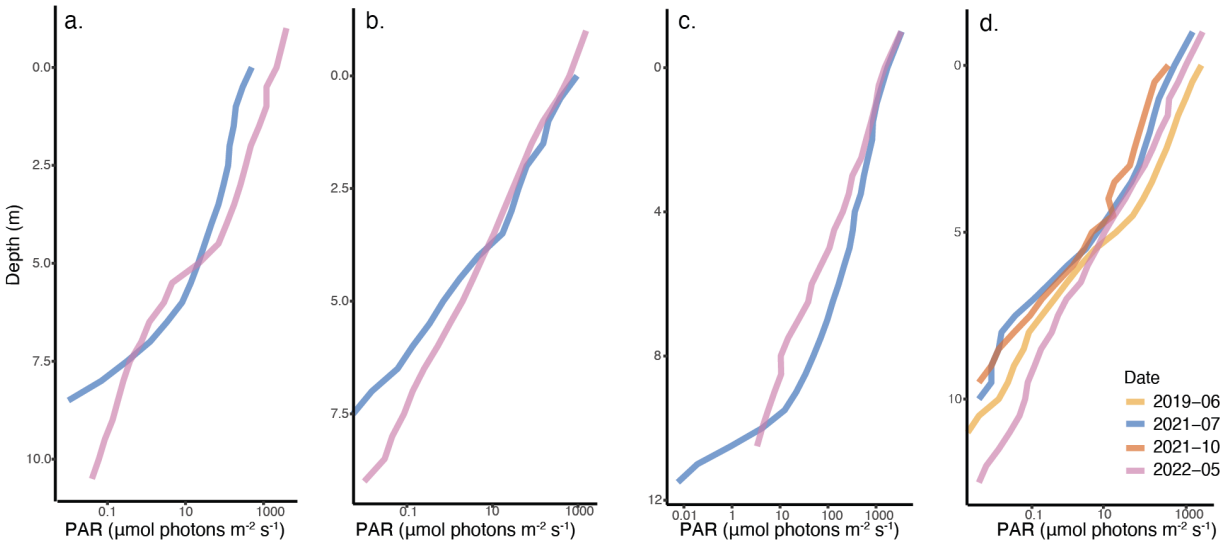

Fig. S15. Photosynthetically active radiation (PAR) profiles of a) Arco Lake, b) Budd Lake, c) Josephine Lake, and d) Deming Lake.

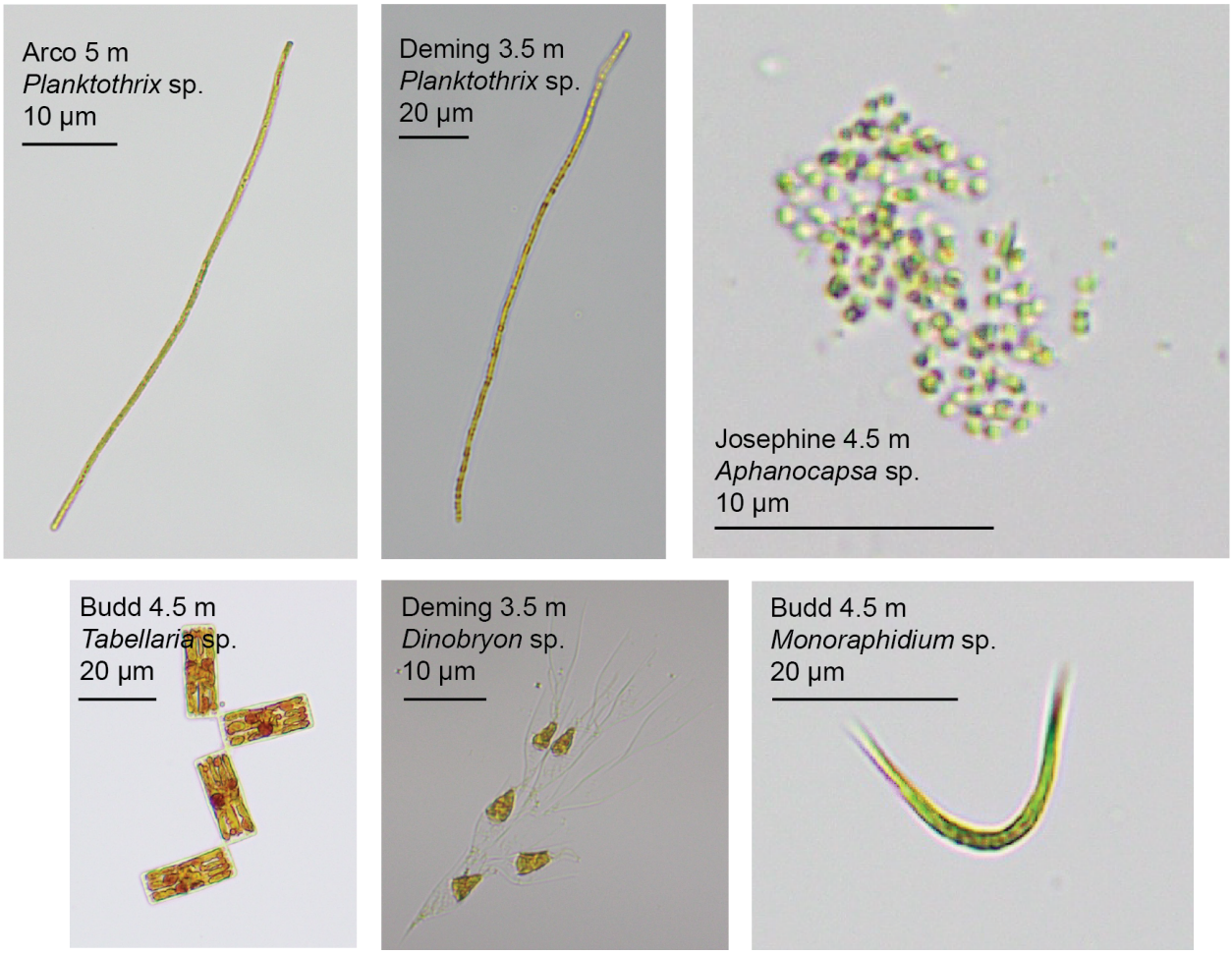

Fig. S16. Cyanobacteria (top row) and eukaryotic algae (bottom row) observed in the study lakes in May 2022.

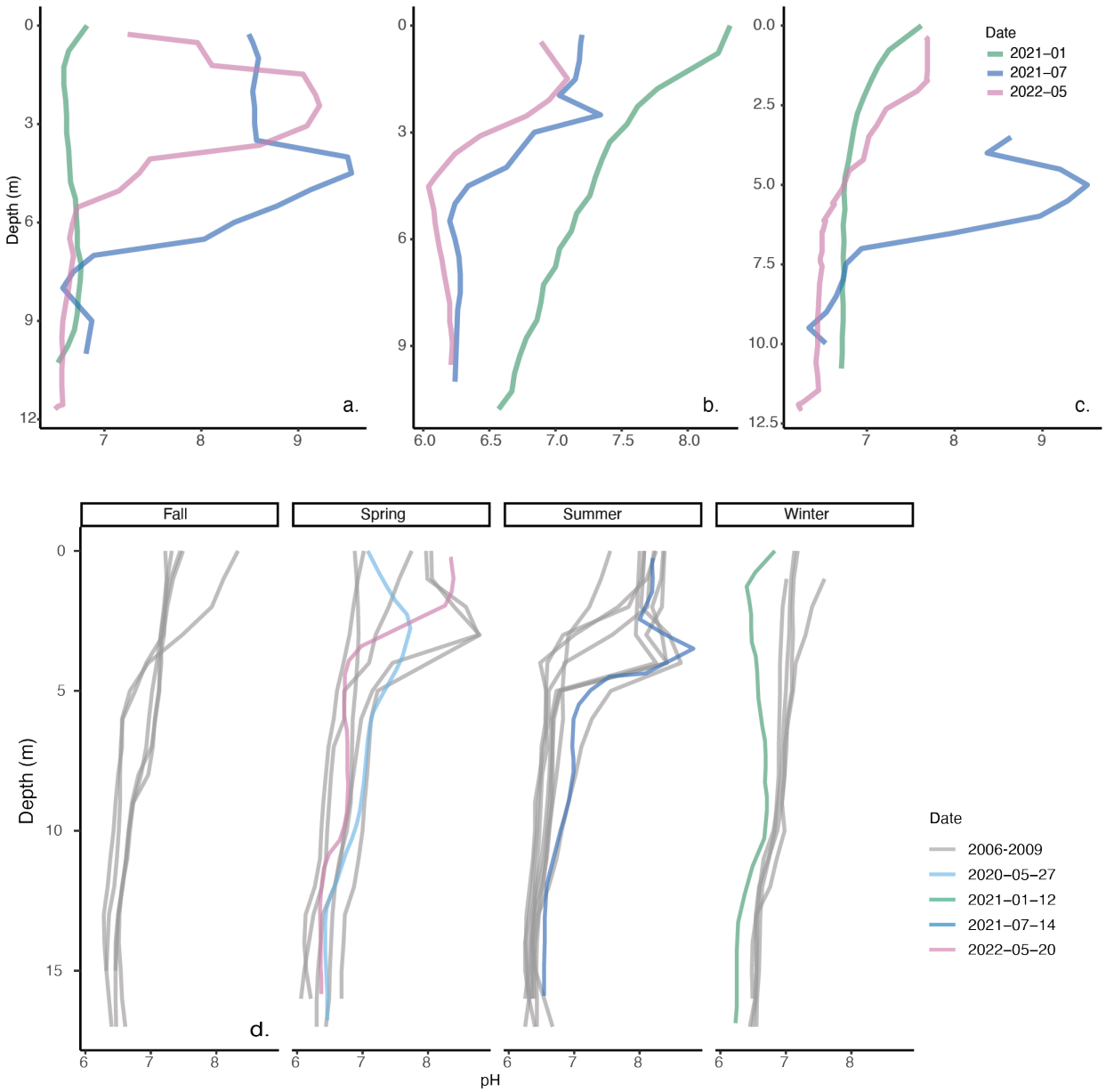

Fig. S18. pH profiles of a) Arco Lake, b) Budd Lake, c) Josephine Lake, and d) Deming Lake. For Deming Lake, seasons were classified according to solstice and equinox dates.

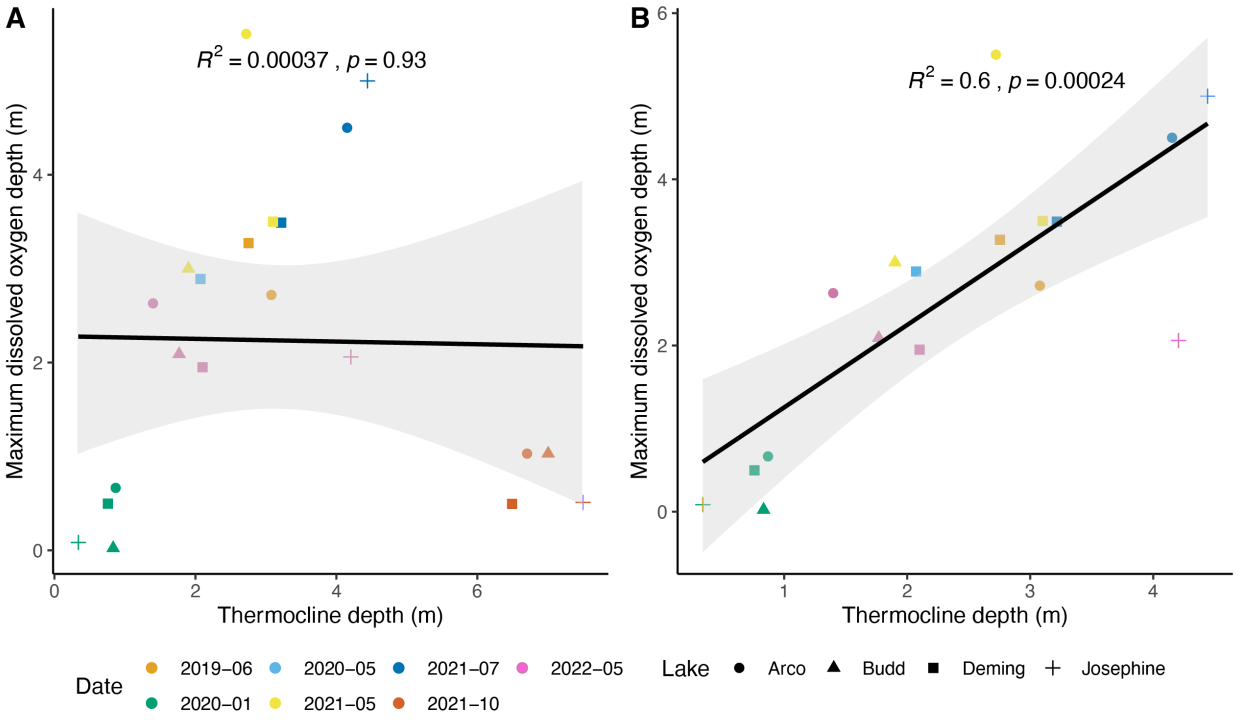

Fig S19. Co-variation between the thermocline depth and the depth of the maximum in dissolved oxygen, and the SCML. Panel A includes data from all dates, and panel B lacks data from October 2021. The correlation is significant when October 2021 datapoints are removed. The grey area is the 95% confidence interval.